PORT SAID ENGINEERING RESEARCH JOURNAL
Faculty of Engineering- Port Said University
Volume (20) No. 2 September 2016 pp: 132:148

Hybrid Desalination System Using Parabolic Trough Concentrator as a Heat Source

Rashed, A.R. [1], *Saif, A.M.*[2], *Shatat, M.M.E.*[3], *and Mohamed, A.M.I.*[4]

ABSTRACT

This paper deals with the status of the new hybrid desalination methods which need more research like thermal vapor compression and direct contact membrane distillation system. The objective of this research is to theoretically investigate the characteristics of a hybrid desalination system composed of a thermal vapor compression (TVC) and direct contact membrane distillation (DCMD) systems using parabolic trough concentrator as a heat source. The proposed hybrid system aims to recover the heat of the rejected brine from thermal vapor compression system in order to obtain the highest fresh water productivity and thermal efficiency and lowest cost of fresh water product from the system. The theoretical simulation of all the systems were developed and solved by Engineering equation solver (EES).

After the validation of all the models, the design of thermal vapor compression and direct contact membrane distillation were selected. It was concluded that the best operating conditions to run the system is at motive steam pressure of 3000 kPa and boiling temperature of 70 ℃. The dynamic behavior of the hybrid system was conducted at the selected operating conditions at different seasons of the year in order to examine the performance of the system through the year. Finally, economic study was developed for the proposed dynamic hybrid desalination system. The results showed that both of the performance ratio and water productivity enhanced by 7.3 % by adding the DCMD as a secondary desalination unit. In addition, the dynamic hybrid system efficiency reached to 75%. Also, the cost of the fresh water product by dynamic hybrid desalination system was 0.0176 $/ L.

Keywords: *Desalination, Hybrid system, Cost analysis.*

1. INTRODUCTION

Water is one of the most important substances on the earth. The Middle East and North Africa (MENA) region is considered as the most water-scarce region of the world. The need for alternative and improved water resources options is a must. Therefore, Desalination of sea water is a very important issue.

Nowadays, some of methods of desalination need more studies and research like thermal vapor compression and membrane distillation. These two types are expected to be more efficient but need further investigations, those also are very interested when we are take about hybrid desalination system.

The main purpose of the hybrid system is to recover the heat of the rejected brine of the Thermal Vapor Compression system (TVC) (high heat reservoir) to be used as a feed solution of the DCMD system (low-level reservoir) to get the maximum possible heat recovery. This is done using parabolic trough concentrators (PTC) as a heat source of all the system.

Literature studies of the TVC desalination system are found by many workers.

A study was presented by A1-Juwayhel, et al.[1] in which a comparison was carried out four for types of single-effect evaporator systems. The systems were thermal vapor compression (TVC), mechanical vapor compression (MVC), absorption vapor compression (ABVC) and adsorption vapor compression (ADVC). The results showed that for TVC the performance ratio increased at high motive steam pressure.

Darwish and El-Dessouky [2] made a comparison of the specific available energy, performance ratio and specific heat transfer area for Multi-Effects Evaporation (MEE), Multi Effect-Thermal Vapor Compression (ME-TVC) and Multi Stage Flash distillation (MSF) systems.

The result showed that the MEE is more efficient from a heat transfer viewpoint than MSF. Also, the ME-TVC system uses less heat transfer surface area compared to MSF and MEE systems for the same energy consumption.

Hamed, et al. [3] compared the exergy losses due to irreversibility of the TVC system with multi-effect boiling (MEB) and the mechanical vapor compression (MVC) systems. The result of this comparison was that the TVC system has the least exergy destruction between the three systems.

Han, et al. [4] developed a new method to improve the entrainment performance of the thermal vapor compressors (TVCs) that was used in multi effect distillation (MED) desalination systems by preheating the entrained vapor by using the heating water from solar system and using steam from an electric boiler as heating source of the entrained vapor preheating.

On the other hand, many literatures studied of membrane distillation systems from the point of heat and mass transfer phenomena and the performance of the DCMD system. Alkhudhiri, et al. [5] introduced a review of all membrane distillation configurations,

[1] *Mechanical Power Engineering Department, Faculty of Engineering, Port Said University, Port Said, Egypt, E-mail: asmaarashed@yahoo.com*
[2] *Mechanical Power Engineering Department, Faculty of Engineering, Port Said University, Port Said, Egypt, E-mail: amanysaif@hotmail.com*
[3] *Mechanical Power Engineering Department, Faculty of Engineering, Port Said University, Port Said, Egypt, E-mail: morsynhomar@yahoo.com*
[4] *Mechanical Power Engineering Department, Faculty of Engineering, Port Said University, Port Said, Egypt, E-mail: mohamed.ay@gmail.com*

characteristics, its applications and its mathematical models.

Schofield, et al. [6] presented a model of the DCMD process. The effects of heat transfer coefficient, membrane permeability and partial pressure of air within the pores were studied. The results of this study showed that the permeate flux could be improved by deaeration.

Termpiyakul, et al. [7] studied the heat and mass transfer on an experimental unit using flat sheet Polyvinylidene Difluoride (PVDF) membrane with pore size 0.22 μm with feed solution of 5000- 35000 mg/L. In this study, it was concluded that the permeate flux was increased with feed temperature and velocity.

Khayet, et al. [8] presented a theoretical model of direct contact membrane distillation taking into account the pore size distribution together with the gas transport mechanisms through the membrane pores. The result of this model was that the predicted water vapor flux increases with the temperature.

Furthermore, many researchers developed several studies about the hybrid desalination systems. Drioli, et al. [9] presented experimental (membrane distillation and reverse osmosis) hybrid system (MD/RO) for water desalination. The MD was proposed to treat the rejected brine from RO with concentration of 75 g/L and temperature of 35℃ because of the MD is less sensitive to the salt concentration. It was found that the productivity of the hybrid system increased twice as much as that produced only by RO.

Hamed [10] presented an overview of the existing hybrid desalination systems, which considered a good economic systems. One of these systems is Hybrid (membrane/thermal/power) configuration which has the advantages of flexibility in operation and less specific energy consumption.

Also, many workers has reviewed many studies about solar collectors and their applications, as that presented by Kalogirou [11], this study provide an overall analysis for different types of solar collectors as presented also by Suman, et al. [12].

Fernandez-Garcia, et al. [13] conducted an overview of a PTCs and its market. Also, presented the current prototypes which under development and its different applications.

The dynamic behavior of the PTC was studied by many researchers. Mohamed [14] described the mathematical model of a parabolic trough collector as a function of three developed partial equations which express the temperature distribution along PTC.

On the other hand, many researchers have provided a number of studies that cover the equations of cost estimation for different desalination configurations. For example, the study provided by Govind and Tiwari [15] which contains economic analysis of different applications of solar systems as solar drying system, solar water heating system, solar distillation units. The estimated cost of mounted single basin still and multiple wick solar still varied from 0.0027 $/kg to 0.0012 $ /kg.

Also, an economical study provided by Elminshawy, et al. [16] for desalination system driven by solar energy. The estimated annual cost was 0.014 $/L for annual desalted product of 18250 L/year.

In the present work the proposed hybrid system consists of TVC as an upper unit and DCMD system using the rejected heat from the upper TVC cycle was analyzed and tested. This hybrid desalination system is driven by parabolic trough concentrators. The performance of such system and its component was estimated theoretically using simulation model from each of thermal and productivity point of views.

2. SYSTEM DESCRIPTION

2.1. TVC system analysis

The Thermal Vapor Compression system (TVC) is a type of conventional thermal desalination process. It consists of evaporator, condenser, steam ejector and heat source. The TVC system depends mainly on the evaporation process which occurs in the evaporator. A schematic diagram of TVC is presented in Fig.1.

The evaporator consists of evaporator/condenser heat section, vapor space, water distribution system and mist eliminator. The condenser type is counter current surface condenser. The steam jet ejector composed of steam nozzle, suction chamber, mixing nozzle and diffuser.

The process of the system is described as follows: The intake seawater (6) is entered to the condenser where it is heated by using a portion of vapor (5) formed by the boiling through the evaporator. A part of heated seawater is used as feed water to the evaporator and the remaining (cooling water) is rejected back to the sea.

The feed water (9) is sprayed at the top of the evaporator, where it falls in the form of a thin film down the succeeding rows of tubes arranged horizontally where the heating steam coming out from the steam jet ejector flows inside the evaporator tubes (3).

Then the mass exit from the steam jet ejector (3) enters to the evaporator, then condenses and exit from the evaporator at points (12, 13). The temperature of boiling inside the evaporator is controlled by the feed water temperature, the available heat transfer area and the overall heat transfer coefficient.

The vapor formed in the evaporator by boiling (4) with a temperature less than the boiling temperature by the boiling point elevation (BPE). The vapor formed flows through wire mesh demister to remove the entrained brine droplets.

Then, the vapor flows from the demister to the condenser where it splits into two portions: The first part (5) condenses outside the tubes of the condenser, while the rest (2) is entrained by the steam jet ejector.

The condensed steam flowing out the evaporator (12) pumped to (15) raising its pressure back to motive steam pressure (P_m). Then the pumped water (15) is heated by the heat source. The water is heated to a temperature equal to the saturated temperature of the motive steam pressure that drives the steam jet ejector. The motive steam (1) is directed at a relatively high pressure into the steam jet ejector.

A part of the vapor formed in the evaporator (2) is entrained and compressed in the steam jet ejector along with the motive steam. Then, the compressed vapor from the steam jet ejector (3) flows through the tubes of the evaporator to heat the feed water (9).

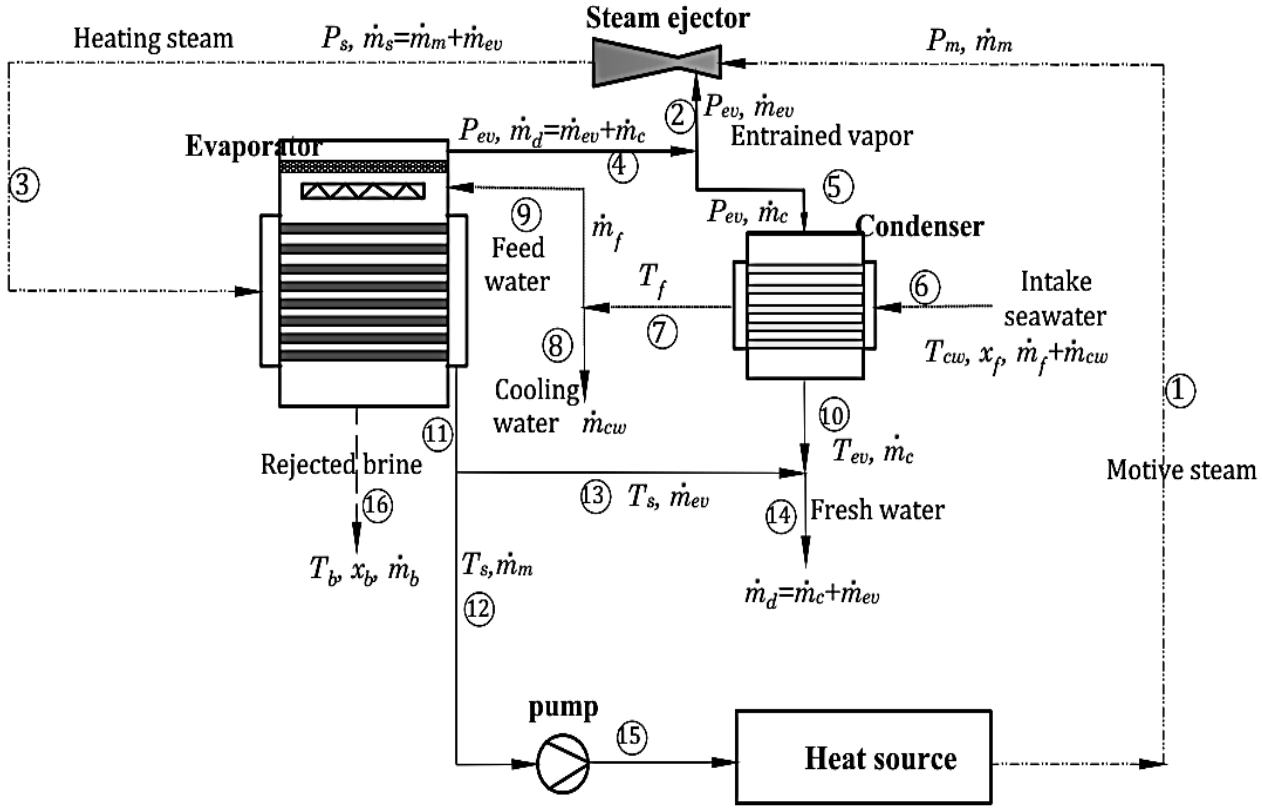

Fig. 1 Flow diagram of Thermal Vapor Compression system

2.2. DCMD System Analysis

Membrane Distillation process is a thermally driven desalination process, which depends on the temperature difference between the two, sides of the membrane (Feed/ Permeate). In the DCMD system the feed solution and the permeate solution become in a direct contact with the hydrophobic membrane as shown in Fig. 2.

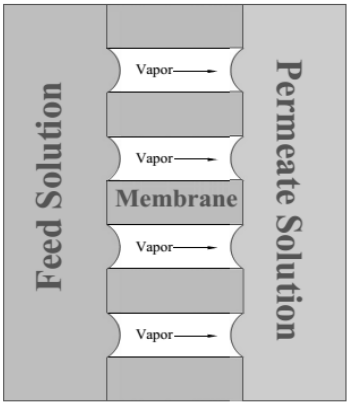

Fig. 2 Direct Contact Membrane Distillation

The hot feed solution and the cold permeate solution are circulated tangentially using circulating pump. Due to the temperature difference between the two sides of the membrane, a pressure difference is established. Because of the pressure difference, the water vapor molecules can now migrate through the membrane pores to the other side comprising the permeate flux.

2.3. PTC System Analysis

PTC is a type of sun tracking concentrating collectors - when temperature range up to 400 ℃ is required, Fig. 3 shows this type. The position of sun is tracked for normal incidence of solar radiations at any instant of time [12]. This collector consists of concentrator and receiver and glass envelop as shows in Fig.4.

The concentrator is a mirror reflector having a shape of cylindrical parabola. It focuses the sunlight onto its axis where it is absorbed on the surface of the receiver tube and transferred to the fluid flowing through it.

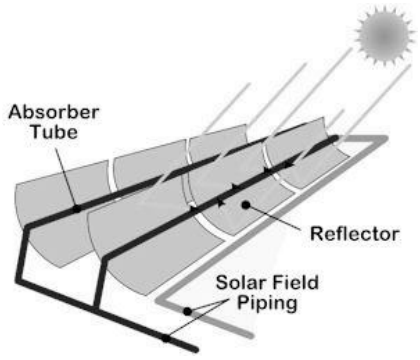

Fig. 3 Parabolic Trough Collector.

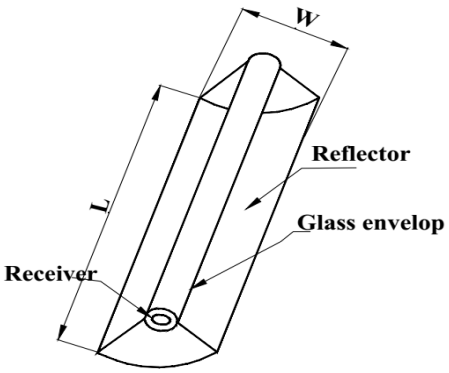

Fig. 4 Components of Parabolic Trough Collector.

2.4. Hybrid TVC/DCMD System Analysis

The hybrid desalination system is a combination between the TVC and DCMD systems. The rejected hot brine from the TVC was used one more time as a feed solution of the DCMD system, this system is driven by dynamic heat source (PTCs) as shown in Fig. 5.

The motive steam is generated in the TVC loop using solar energy (PTC). The total distilled water productivity is related to the operating conditions of both TVC and DCMD systems.

3. MATHEMATICAL FORMULATIONS

3.1. Mathematical Model of TVC system

The mathematical model of the TVC system includes energy and mass balance equations for the evaporator, condenser, and steam ejector. Analysis of the TVC system focuses on evaluation of the system variables, which affect the TVC system performance.

By applying a mass balance of the system:

$$\dot{m}_f = \dot{m}_b + \dot{m}_d \quad (1)$$

$$\frac{\dot{m}_d}{\dot{m}_f} = \frac{x_b - x_f}{x_b} \quad (2)$$

Where $\dot{m}_f, \dot{m}_b \; and \; \dot{m}_d$ (kg/s) are the mass flow rate of feed water, brine and distillate, respectively and x_b, x_f (ppm) are the salinity of brine and feed water, respectively. Then, by applying a heat balance on the evaporator:

$$\dot{Q}_e = \dot{m}_s \lambda_s \quad (3)$$

$$\dot{Q}_e = \dot{m}_f \, c_{pb}\left(T_b - T_f\right) + \dot{m}_d \lambda_d \quad (4)$$

Where:

$$\dot{m}_s = \dot{m}_m + \dot{m}_{ev} \quad (5)$$

Where $\dot{Q}_e$ is the evaporator heat transfer rate (kW), $\dot{m}_s$ is the heating steam flow rate (kg/s), λ_s is the corresponding heating steam latent heat (kJ/kg), c_{pb} is the brine specific heat $(kJ//kg.℃)$, T_b is the boiling temperature (℃), T_f is the feed water temperature (℃), λ_d is the vapor latent heat (kJ/kg), $\dot{m}_m$ is the motive steam mass flow rate and $\dot{m}_{ev}$ is the entrained vapor mass flow rate in (kg/s). Both of the specific heat and the latent heat can be obtained from empirical correlations [17] as a function of saturation temperature and water salinity. The generated vapor is at the saturation temperature T_v, which corresponds to the pressure in the evaporator vapor space. This temperature is less than the boiling temperature T_b by the boiling-point elevation BPE.

$$T_v = T_b - BPE \quad (6)$$

Boiling Point Elevation (BPE) is calculated from an empirical formula as a function of boiling temperature [17]. Then the evaporator heat transfer surface area, A_e, can be obtained from:

$$A_e = \frac{\dot{Q}_e}{U_e(T_s - T_b)} \quad (7)$$

Where T_s is the heating steam temperature (℃), U_e is the overall heat transfer coefficient of the evaporator $(kW/m^2.℃)$. The condensation temperature of vapor in the condenser (T_c) is less than the boiling temperature in the evaporator (T_b) by the boiling point elevation (BPE) and the saturation temperature decreased according to the pressure losses in demister the (ΔT_p)

$$T_c = T_b - \left(BPE + \Delta T_p\right) \quad (8)$$

Where ΔT_p is the saturation temperature corresponding to the pressure drop in the demister pad. The pressure loss in the demister pad can be obtained from a correlation given by El-Dessouky and Ettouney [17]. Then by applying a heat balance on the condenser:

$$\dot{Q}_c = \dot{m}_c \, \lambda_c \quad (9)$$

$$\dot{Q}_c = \left(\dot{m}_{cw} + \dot{m}_f\right) c_{pf}\left(T_f - T_{cw}\right) \quad (10)$$

Then the condenser heat transfer surface area, A_c, can be obtained from:

$$A_c = \frac{\dot{Q}_c}{U_c (LMTD)_c} \quad (11)$$

Where:

$$\dot{m}_c = \dot{m}_d - \dot{m}_{ev} \quad (12)$$

Where $\dot{Q}_c$ is the condenser heat transfer rate (kW), T_f and T_{cw} are the feed and seawater temperatures (℃), respectively, λ_c is the latent heat corresponding to water vapor temperature T_v in (kJ/kg), c_{pf} is the specific heat of feed water in $(kJ//kg.℃)$, $\dot{m}_{cw}$ is the cooling water flow rate (kg/s) $\dot{m}_c$ is the inlet water vapor mass flow rate into the condenser in (kg/s), U_c is the overall heat transfer coefficient of the condenser $(kW/m^2.℃)$ and $(LMTD)_c$ is the logarithmic mean temperature difference (℃) and can be calculated from:

$$(LMTD)_c = \frac{T_f - T_{cw}}{ln(T_c - T_{cw})/(T_c - T_f)} \quad (13)$$

Both of the overall heat transfer coefficient of the evaporator and condenser, $(U_e \; and \; U_c)$ can be calculated by El-Dessouky and Ettouney empirical correlations [18].

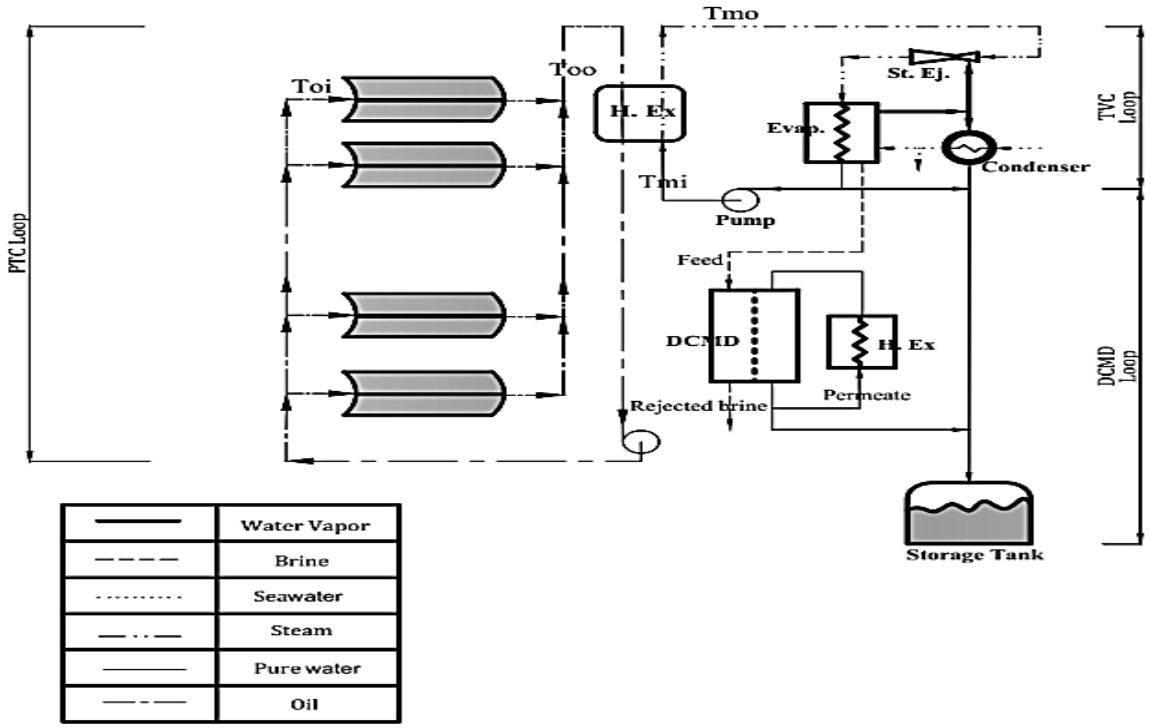

Fig. 5 Flow diagram of Hybrid desalination system driven by solar energy (PTC).

Steam Ejector Equations:

The compression ratio of the steam ejector is defined as the ratio of the heating steam pressure, P_s, to the entrained vapor pressure, P_{ev}.:

$$CR = \frac{P_s}{P_{ev}} \quad (14)$$

While, the entrainment ratio is defined as the motive steam, $\dot{m}_m$,to the entrained vapor mass flow rate, $\dot{m}_{ev}$:

$$Ra = \frac{\dot{m}_m}{\dot{m}_{ev}} \quad (15)$$

In the present study, with steam is the motive fluid , for pressure range of $500 \geq P_m \geq 1500\ (kPa)$, the equation used to calculate the entrainment ratio is predicted by [17]–[19].

For the range of $1500 \geq P_m \geq 2000\ (kPa)$, the equation used to calculate the entrainment ratio is predicted using DataFit version 9.x [20].

$$Ra = 0.915 * \frac{(P_s)^{1.091}}{(P_{ev})^{0.887}} * \left(\frac{P_m}{P_{ev}}\right)^{-0.2496} \quad (13)$$

The results from this equation are compared with the power graphical method and give a good agreement for the given range of motive steam pressure. For the range of $2000 \geq P_m \geq 3000\ (kPa)$. The equation used to calculate the entrainment ratio is predicted by [21], [22], as:

$$Ra = 0.235 * \frac{(P_s)^{1.19}}{(P_{ev})^{1.04}} * \left(\frac{P_m}{P_{ev}}\right)^{0.015} \quad (17)$$

The performance of the TVC system is measured by the following variables:

- The performance ratio is defined as the ratio of the distillate water, $\dot{m}_d$, mass flow rate to motive steam mass flow rate:

$$PR = \frac{\dot{m}_d}{\dot{m}_m} \quad (18)$$

- The specific heat transfer surface area is defined as the ratio of the total heat transfer area of the condenser and evaporator to the distillate water mass flow rate:

$$SA = \frac{A_e + A_c}{\dot{m}_d} \quad (19)$$

- The specific cooling water mass flow rate is defined as the ratio of the cooling water mass flow rate to the distillate water mass flow rate:

$$SM_{cw} = \frac{\dot{m}_{cw}}{\dot{m}_d} \quad (14)$$

The design data used in the TVC calculations are given in Table 1.

3.2. Mathematical Model of DCMD system

In DCMD process, both heat and mass transfer through porous hydrophobic membranes are involved simultaneously. The mass transfer occurs through the pores of the membrane whereas heat is transferred through both the membrane and its pores. The heat transfer through the direct contact membrane is described by three steps illustrated in Fig. 6.

Table 1: Input data to the mathematical model of TVC

Data	Value	Unit
Boiling temperature, T_b	50 to 70	℃
Seawater temperature, T_{cw}	25	℃
Density of demister pad material, ρ_p	375	kg/m^3
Ejector compression ratio, CR	2 to 5	
Feed sea water temperature, T_f	$T_b - 5$	
Feed seawater salinity, x_f	42000	ppm
Distillate water, $\dot{m}_d$	1	kg/s
Maximum brine salinity, x_b	70000	ppm
Motive steam pressure, P_m	500 to 3000	kPa
Thickness of demister pad, L_p	0.1	m
Vapor velocity in demister pad, V_p	6	m/s
Wire diameter of demister pad, δ_w	0.28	mm

Heat Transfer through the Feed Side:

The heat transfer through the feed aqueous solution of the DCMD unit is a convective heat transfer rate and is calculated as follows:

$$\dot{Q}_f = h_f \, A_m \left(T_{bf} - T_{mf}\right) \qquad (15)$$

Where h_f is the heat transfer coefficient $(kW/m^2.℃)$, A_m is the effective membrane area (m^2) can be calculated from Table. 2, T_{mf} is the membrane feed side temperature (℃) and T_{bf} is the bulk feed temperature (℃) which is equal to $\left(T_{bfi} + T_{bfo}\right)/2$. At steady state, the convective heat transfer rate must equal the rejected flow energy of the feed solution which can be expressed as:

$$\dot{Q_f} = \dot{m}_{fmd} \, cp_{bf} \left(T_{bfi} - T_{bfo}\right) \qquad (16)$$

Where $\dot{m}_{fmd}$ is the feed mass flow rate (kg/s), cp_{bf} is feed specific heat transfer $(kJ/kg.℃)$and can be calculated from EES seawater library, T_{bfi} is the inlet bulk feed temperature (℃), T_{bfo} is the outlet bulk feed temperature (℃). The heat transfer coefficient of the feed side can be calculated from the following relation:

$$Nu_f = \frac{h_f \, D_h}{k_{bf}} \qquad (23)$$

$$Re = \frac{\rho * V * D_h}{\mu} \qquad (24)$$

Where Nu_f is the feed Nusselt number, Re is Reynolds number, k_{bf} is the thermal conductivity of the feed aqueous solution $(kW/m.℃)$ and can be calculated from EES seawater library, D_h is the hydraulic diameter of the rectangular cross sectional channel *(m)*, Re is Reynolds number, ρ is the density of the flow, V is the velocity of the flow through the channel and μ is the dynamic viscosity $(kg/m.s)$. The Nusselt number can be calculated by using empirical equations for turbulent $(Re > 2300)$and laminar flow $(Re < 2300)$ which are given in Table.2.[23]

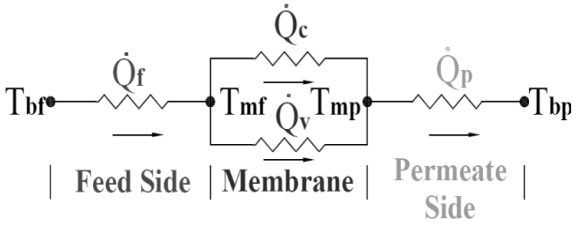

Fig. 6 Heat Transfer through DCMD System

Heat transfer through the membrane:

The total heat flux through the membrane, $\dot{Q}_m$, is due to two mechanisms:

- Conduction across the membrane,$\dot{Q}_c$.
- Latent heat associated with the vaporized molecules, $\dot{Q}_v$.

The heat transfer due to the latent heat of vapor molecules can be calculated as:

$$\dot{Q}_v = J_w \, \Delta H_v A_m \qquad (25)$$

Where J_w is the permeate flux through the membrane pores $(kg/m^2.s)$ and can be calculated by Eq. (32) and $\Delta H_v$is the latent heat of evaporation associated with the migration of the water vapor molecules through the membrane pores and can be calculated at the mean membrane temperature, $T_m = T_{mf} + T_{mp}/2$, [7], [24], [25]. In addition, the heat transfer rate of conduction can be calculated as follows:

$$\dot{Q}_c = \frac{K_m}{\delta_m} \left(T_{mf} - T_{mp}\right) A_m \qquad (26)$$

Where K_m is the membrane thermal conductivity $(kW/m^2.℃)$ and δ_m is the membrane thickness (m).

Heat Transfer through the Permeate Side:

The heat transfer mechanism in the permeate side is a convective heat transfer type and can be calculated from:

$$\dot{Q}_p = h_p \, A_m \left(T_{mp} - T_{bp}\right) \qquad (27)$$

Where h_p is the heat transfer coefficient of the permeate side $(kW/m^2.℃)$, T_{mp} is the membrane permeate side temperature (℃) and T_{bp} is the bulk permeate temperature (℃) which is equal to $\left(T_{bpi} + T_{bpo}\right)/2$. At steady state, the convective heat transfer rate through the permeate side of the membrane is equal to the flow energy of the permeate side:

$$\dot{Q}_p = \dot{m}_{pmd} \, cp_{bp} \left(T_{bpo} - T_{bpi}\right) \qquad (28)$$

Where $\dot{m}_{pmd}$ is the permeate mass flow rate (kg/s), cp_{bp} is permeate specific heat transfer $(kJ/kg.℃)$and can be calculated from EES water library, T_{bpi} is the inlet bulk permeate temperature (℃), T_{bpo} is the outlet bulk permeate temperature (℃). So, the total heat flow through the membrane can be expressed as:

$$\dot{Q} = U_m \, A_m \Delta T \qquad (29)$$

Where:

$$U_m = \left[\frac{1}{h_f} + \frac{1}{k_m/\delta + J_w\,\Delta H_v/\Delta T_m} + \frac{1}{h_p}\right]^{-1} \quad (30)$$

Where $U_m(kW/m^2.℃)$ is the total heat transfer coefficient through the membrane module.

Mass transfer through the membrane:

In the DCMD process, the mass transport is usually described by assuming a linear relationship between the mass flux (J_w) and the water vapour pressure difference through the membrane (Δp_w) [8], [26]–[30] and can be expressed as follow:

$$J_w = B_m \Delta p_w \quad (31)$$

$$= B_m\left(P_{mf} - P_{mp}\right)$$

Where B_m is the permeability of the membrane $(kg/m^2.\mathrm{s.Pa})$, P_{mf} is the partial pressure of water vapor at the feed side of the membrane (Pa) and P_{mp} is the partial pressure of water vapor at the permeate side of the membrane (Pa).The partial pressures of water at the feed and permeate sides evaluated by using Antoine equation at the temperatures T_{mf} and T_{mp}, respectively, such as the following [2], [3]:

$$P^v = exp\left(23.328 - \frac{3841}{T-45}\right) \quad (32)$$

Where T is in K. For combined Knudsen ordinary diffusion mechanism $\left(0.5\lambda_w < r_p < 50\lambda_w\right)$:

$$B_m = \frac{1}{RT\delta_m} * \left(\frac{3\tau}{2\varepsilon\, r_p} * \left(\frac{\pi M_w}{8RT}\right)^{0.5} + \frac{P_a \tau}{\varepsilon PD}\right)^{-1} \quad (33)$$

Where ε is the membrane porosity, r_p is the membrane pore radius (m), R is the universal gas constant $(kJ/kmole.k)$, T is the mean temperature through the membrane pores (K), τ is the membrane tortuosity, M_w is the molecular weight of water vapor $(kg/kmole)$ and P_a is the average air pressure usually taken equal to 1 bar, and PD is the diffusivity of water vapor through the stagnant air inside the pores and can be calculated as follows:

$$PD = 1.895 * 10^{-5} T^{2.072} \quad (34)$$

The performance of the DCMD system is measured by the following variables:

- Temperature Polarization Coefficient (TPC) is generally used to quantify the magnitude of the boundary layer resistances over the total heat transfer resistance:

$$TPC = \frac{T_{mf} - T_{mp}}{T_{bf} - T_{bp}} \quad (35)$$

- DCMD efficiency is defined as the heat of evaporation divided to the total heat input to the system:

$$\eta = \frac{J_w\,\Delta H_V\,A_m}{\dot{Q}} \quad (36)$$

The present DCMD module consists five stages are arranged in series each stage consists of a number of flat sheet (Polyvinylidene Difluoride) PVDF membranes that are assembled in parallel, forming a number of flow channels for the feed and permeate to flow at two sides of the membranes. Each flow stream within the channels is in direct contact with one side of five membranes with total membrane area of $11.25\ m^2$. The design data used in the DCMD calculations are given in Table 3.

Table 2: Empirical Equations of heat transfer for DCMD

Empirical Equations	Flow Type
$Nu = 0.13 * Re^{0.64} * Pr^{0.38}$	Laminar
$Nu = 0.027 * Re^{4/5} * Pr^{m} * \left(\frac{\mu_b}{\mu_m}\right)^{0.14}$	Turbulent

Where The superscript m is 0.4 for heating and 0.3 for cooling; μ_b and μ_m are the water dynamic viscosity at the bulk and at the membrane surface.

Table 3: Input Data to the mathematical model of the DCMD

Data	Value	Unit
Thickness of the membrane, δ_m	126	μm
Thermal conductivity of the membrane, k_m	0.041	$W/m.K$
Porosity, ε	0.75	
Pore diameter, d_p	0.22	μm
Inlet bulk feed temperature, T_{bfin}	50 to 70	℃
Inlet bulk permeate temperature, T_{bpin}	25	℃
Salinity of the feed solution, x_f	70,000	ppm
Velocity of the permeate, V_{pmd}	1.5	m/s
Hydraulic diameter of the membrane, D_h	0.004	m
Tortuosity of the membrane, τ	1	
Width of the channel, w	0.3	m
Length of the membrane, L	1.5	m
Total membrane area, $A_m = L * w * 5 * 5$	11.25	m^2

3.3. Mathematical Model of PTC

Mathematical model solution of the Parabolic trough solar collector is basically depending on three energy equation of fluid element, receiver tube and finally the glass cover. Fig. 7 shows a cross section of PTC. The model had been developed and validated by Mohamed [14]. The energy equation of the fluid element can be expressed as follows:

$$\frac{\partial T_f}{\partial t} + V.\frac{\partial T_f}{\partial x} = \frac{\alpha_{rf}.\pi.D_{ri}.(T_r - T_f)}{\rho_f.A_f.c_{pf}} \quad (37)$$

The initial and boundary conditions to solving the previous equation are:

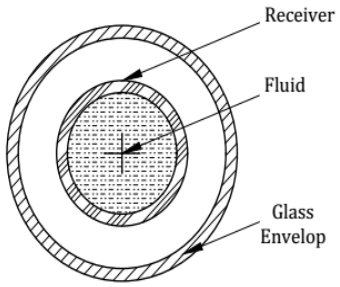

Fig. 7 Cross Section of Parabolic Trough Collector.

$$T_f(x, t = 0) = T_a \quad (38)$$

$$T_f(x = 0, t) = T_{fi} \quad (39)$$

Where T_f is the fluid temperature, D_{ri} is the inner diameter of the receiver, T_r is the receiver temperature, ρ_f is the fluid density, c_{pf} is the specific heat of the fluid, t is time, T_{fi} is the inlet fluid temperature, T_a is the ambient fluid temperature, V is the flow velocity and A_f is the flow area and can be calculated from:

$$A_f = \pi \, . D_{ri}^2 \quad (40)$$

The convection heat transfer coefficient, α_{rf}, can be calculated from the following equation:

$$\alpha_{rf} = \frac{Nu * k_f}{D_{ri}} \quad (41)$$

Where k_f is the thermal conductivity of the fluid, Nu is the Nusselt number can be calculated from the following table:

Table 4: Empirical Equations of heat transfer for PTC

Empirical Equations	Flow Type
$Nu = 3.66 + \frac{0.065 * (D_{ri}/L) * Re * Pr}{1 + 0.04[(D_{ri}/L) * Re * Pr]^{2/3}}$	Laminar
$Nu = \frac{(f/8) * (Re - 1000) * Pr}{1 + 12.7 * (f/8)^{0.5} * (Pr^{2/3} - 1)}$	Turbulent

Where L is the receiver length, f is the friction factor, Re is Reynolds number and Pr is Prandtl number. Also, the energy equation for the receiver can be expressed as follows:

$$\frac{\partial T_r}{\partial t} - a_r . \frac{\partial^2 T_r}{\partial x^2} = \frac{I_o . D_{ro} . ab_r . \gamma . \tau_{cover} . \tau_{egc} . CF_r}{\frac{(D_{ro}^2 - D_{ri}^2)}{4} \rho_r \, . c_{pr}} - \frac{\alpha_{rg} . D_{ro} . (T_r - T_g)}{\frac{(D_{ro}^2 - D_{ri}^2)}{4} \rho_r \, . c_{pr}} - \frac{\alpha_{rf} . D_{ri} . (T_r - T_f)}{\frac{(D_{ro}^2 - D_{ri}^2)}{4} \rho_r \, . c_{pr}} \quad (42)$$

The initial and boundary condition of this equation are:

$$T_r(x, t = 0) = T_a \quad (43)$$

$$\frac{\partial T_r}{\partial x}\Big)_{(x=0,t)} = \frac{\partial T_r}{\partial x}\Big)_{(x=L,t)} = 0 \quad (44)$$

Where ab_r is the absorptivity of the receiver, D_{ro} is the outer diameter of the receiver, a_r is the receiver thermal diffusity, γ is the correction factor of the diffuse radiation, τ_{cover} is the transmissivity of the glass envelop, τ_{egc} is the effective transmissivity of glass envelop, CF_r is the concentration ratio of the receiver and can be calculated from Eq. (45), I_o is the intensity of the solar radiation falling on it (W/m^2), ρ_r is the receiver density, c_{pr} is the specific heat of the receiver, T_g is the glass envelop temperature and α_{rg} is the combined heat transfer coefficient between the receiver and the glass envelop and can be calculated from Eq. (46).

$$CF_r = \frac{w * L}{\pi * D_{ro} * L} \quad (45)$$

Where w is the collector width.

$$\alpha_{rg} = \alpha_{rad} + \alpha_{conv} \quad (46)$$

When the collector annulus is under vacuum, $\alpha_{conv} = 0$. So, the heat transfer coefficient due to radiation only, α_{rad}, can be calculated from the following relation:

$$\alpha_{rad} = \frac{\sigma * \left(T_g{}^2 + T_r{}^2\right) * \left(T_g + T_r\right)}{(1/\varepsilon_r) + (D_{or}/D_{ig}) * (1/\varepsilon_g - 1)} \quad (47)$$

Where ε_r is the emissivity of the receiver, ε_g is the emissivity of the glass envelop and σ is the Stefan Boltzmann constant and is equal to $5.67 * 10^{-8}$ $(W/m^2.K^4)$. Finally, the energy equation of the glass envelop:

$$\frac{\partial T_g}{\partial t} - a_g . \frac{\partial^2 T_g}{\partial x^2} = \frac{I_o . D_{go} . ab_g . \gamma . \tau_{egc} . CF_g}{\frac{(D_{go}^2 - D_{gi}^2)}{4} \rho_g \, . c_{pg}} - \frac{\alpha_{rg} . D_{gi} . (T_r - T_g)}{\frac{(D_{go}^2 - D_{gi}^2)}{4} \rho_g \, . c_{pg}} - \frac{\alpha_{ga} . D_{go} . (T_g - T_a)}{\frac{(D_{go}^2 - D_{gi}^2)}{4} \rho_g \, . c_{pg}} \quad (48)$$

The initial and boundary condition of this equation are:

$$T_g(x, t = 0) = T_a \quad (49)$$

$$\frac{\partial T_g}{\partial x}\Big)_{(x=0,t)} = \frac{\partial T_g}{\partial x}\Big)_{(x=L,t)} = 0 \quad (50)$$

Where ab_g is the absorptivity of the glass, D_{go} is the outer diameter of the glass, a_g is the glass thermal diffusity D_{gi} is the inner diameter of the glass envelop, CF_g is the concentration ratio of the glass and can be calculated from Eq. (51), ρ_g is the glass density, c_{pg} is the specific heat of the glass and α_{ga} is the combined heat transfer coefficient between the glass envelop and the ambient and can be calculated from Eq. (52).[23]

$$CF_g = \frac{w * L}{\pi * D_{go} * L} \quad (51)$$

$$\alpha_{ga} = \alpha_{rad} + \alpha_{conv} \quad (52)$$

$$\alpha_{rad} = \varepsilon_g * \sigma * \left({T_g}^2 + {T_{sky}}^2\right) * \left(T_g + T_{sky}\right) \quad (53)$$

$$\alpha_{conv} = \frac{Nu * k_a}{D_{go}} \quad (54)$$

$$Nu = y * {Re_g}^m * {Pr_a}^n * \left(\frac{Pr_a}{Pr_g}\right)^{1/4} \quad (55)$$

The superscript, n is equal:

$$n = 0.37, for\ Pr_a \leq 10$$
$$n = 0.36, for\ Pr_a > 10$$

Table 5: Constants of Eq.(55)

Re_g	y	m
1-40	0.75	0.4
40-1000	0.51	0.5
1000-200000	0.26	0.6
200000-1000000	0.076	0.7

Where T_{sky} is the sky temperature. The performance of the PTC is measured by the its efficiency, which equal to the useful heat output at any instant to the input heat at the same instant, and given by:

$$\eta_{PTC} = \frac{\dot{m}.c_{Pf}.(T_{fo} - T_{fi})}{I_O.A_{col}} \quad (56)$$

Where $\dot{m}$ is the oil mass flow rate, T_{fo} is the outlet oil temperature and A_{col} is the collector area. The mathematical model of the PTC is solved using the data given in Table 6.

3.4. Mathematical Model of the Hybrid Desalination system

The mathematical model of the hybrid system consists of the three system analysis discussed so far. The rejected energy from the TVC is transferred to the DCMD.

The performance of the Hybrid desalination system is measured by:

- Performance ratio of the Hybrid desalination system, which is the ratio of the total distillate water flow rate, $\dot{m}_{dt}$, to the motive steam flow rate, $\dot{m}_m$.

$$PR_{hy} = \frac{\dot{m}_{dt}}{\dot{m}_m} \quad (57)$$

- Efficiency of the hybrid system: is ratio of the total distillate water from the system multiplying by the latent heat of water at 1 bar, ΔH_v, to the total heat input to the system, and expressed as follows:

$$\eta_{sys} = \frac{\dot{m}_{dt}.\Delta H_v}{\sum I_O.A_{col}} \ \% \quad (58)$$

Where $\sum A_{col}$ is the total collector area and can be calculated as follows:

$$\sum A_{col} = no.of\ collectors * L * w = 867 * 5 * 1.9 = 8236.5\ m^2 \quad (59)$$

Table 6: Design Data of PTC

Data	Value	Unit
Collector length, L	5	m
Collector aperture width, w	1.9	m
Collector Area, A_{col}	9.5	m^2
Inner diameter of receiver, D_{ri}	20	mm
Outer diameter of receiver, D_{ro}	22	mm
Inner diameter of glass cover, D_{gi}	40	mm
Outer diameter of glass cover, D_{go}	45	mm
Receiver absorptivity, ab_r	0.9	
Receiver emissivity, ε_r	0.1	
Glass envelop absorptivity, ab_g	0.15	
Glass envelop emissivity, ε_g	0.88	
Glass envelop transmissivity, τ_g	0.85	
Correction factor of diffuse radiation, γ	0.95	
Concentration ratio, CF_r	27	
Wind velocity, C_{wind}	4	m/s
Ambient temperature, T_a	20	℃
Thermal conductivity of receiver, k_r	$151 * 10^{-3}$	kW/m. K
Thermal conductivity of glass envelop, k_g	$1 * 10^{-3}$	kW/m. K
Density of receiver material, ρ_r	$8.8 * 10^3$	kg/m^3
Density of glass envelop, ρ_g	2700	kg/m^3
Specific heat of receiver, c_{pr}	0.38	kJ/kg. K
Specific heat of glass envelop, c_{pg}	0.84	kJ/kg. K
Mass flow rate of oil inside one PTC, $\dot{m}$	0.005	kg/s

3.5. Solution Procedure of TVC, DCMD and PTC Systems

The solution procedure of all the systems are solved according to the equations stated earlier. The solution of the systems was done using Engineering Equation Solver (EES). EES is a powerful tool for solving simultaneous equations using iterative method

Also, it's particularly useful in solving thermodynamic and heat transfer problems since it offers several built-in libraries comprising of thermodynamic and thermo physical properties. On the other hand, the theoretical model of parabolic trough collector is basically depending

on three energy equations of the fluid element, absorber and glass cover.

Every energy equation is solved by finite difference method (Crank -Nicklson method) in order to convert it to the linear form. Then, these equations were solved according to Tri-diagonal matrix algorithm for every time step.

. MODELS VALIDATION

4.1. TVC Model Validation

In order to validate the simulation results obtained from the present TVC model, a comparison has been held with the previous theoretical results of Al-Juwayhel, et al. [1] at the same operating conditions.

Fig. 8 shows the effect of boiling temperature on the performance ratio at different values of motive steam pressure for both the present model results and Al-Juwayhel, et al. [1] theoretical results.

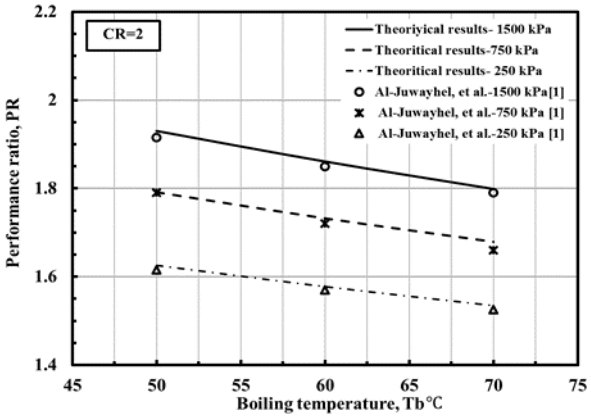

Fig. 8 Comparison between the present model results and Al-Juwayhel, et al. [1] results of the performance ratio as a function of the boiling temperature and the motive steam pressure.

While, Fig. 9 presents the effect of boiling temperature on the specific heat transfer area of the TVC system at different values of motive steam pressure for both the present model results and Al-Juwayhel, et al. [1] theoretical results.

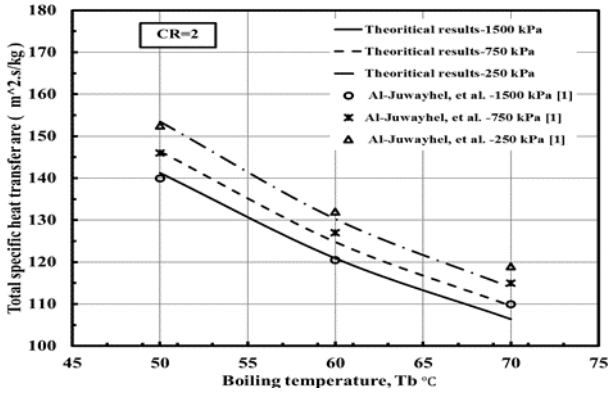

Fig. 9 Comparison between the present model results and Al-Juwayhel, et al. [1] results of the specific heat transfer area as a function of the boiling temperature and the motive steam pressure.

A good agreement was obtained for the comparison of the present model results and Al-Juwayhel, et al. [1] theoretical results for different parameters. However, the maximum difference between the two results was about 5.2 %.

4.2. DCMD Model Validation

This part is interested in holding a comparison between the present theoretical results of DCMD model and the experimental results obtained by Termpiyakul, et al.[7] at the same operating conditions.

The following Fig. 10 describes the comparison between the present model results and the Termpiyakul, et al. [7] results of permeate flux obtained, respectively as a function of the feed temperature of the feed solution.

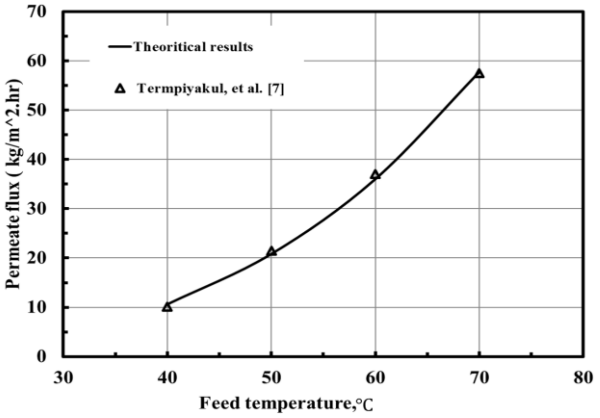

Fig. 10 Comparison between the present model results and Termpiyakul, et al. [7] results of the permeate flux as a function of the feed temperature.

Finally, Fig. 11 holds a comparison between the present model results and Termpiyakul, et al. [7] results of the temperature polarization coefficient as a function of feed temperature.

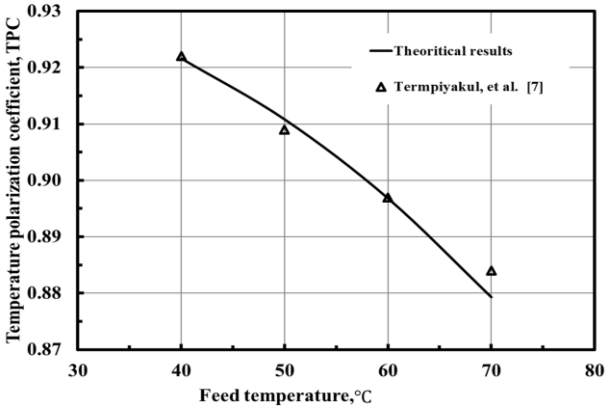

Fig. 11 Comparison between the present model results and Termpiyakul, et al. [7] results of the temperature polarization coefficient as a function of the feed temperature.

From the previous comparisons, it is noticed a good agreement between the present model results and the results obtained by Termpiyakul, el al. [7] where the maximum diference between the two results was 3.5%.

5. RESULTS AND DISCUSSION

This section presents the theoretical results in studying the performance and characteristics of TVC, DCMD and Hybrid systems. Firstly, The TVC system is studied with fresh water productivity of 1 kg/s. The study considers changing of operating conditions: boiling temperature T_b (50 to 70 ℃) motive steam pressure P_m (500 to 3000 kPa) and compression ratio Cr (2 to 5).

The performance ratio, the specific heat transfer area and specific cooling water flow rate are the comparative parameters studied for different operating conditions. After that, the hybrid desalination system using steady heat source is studied under different operating conditions of boiling temperature T_b ,and motive steam pressure P_m.

Meanwhile, the hybrid system driven by steady heat source is tested for different operating conditions, varying the boiling temperature T_b ,and motive steam pressure P_m.

Finally, the dynamic hybrid system was run for different months of the year of January, April, July and October. Every month of the year was run at the previous selected design conditions. The performance of the system was investigated in terms of solar collector efficiency, performance ratio of the hybrid system, thermal efficiency of the hybrid system and the total water productivity obtained in a certain day of each month of the year.

5.1. Hybrid Desalination System Driven by Steady Heat Source

Firstly, the theoretical model of the TVC system for the design shown in Fig. 1 was solved for the input data shown in Table.1. The results obtained from this solution are corresponding to 1 kg/s of fresh water productivity.

It can be concluded that, in order to obtain higher performance ratio, higher productivity and lower energy consumption, higher motive steam pressure, moderate boiling temperature and lower compression ratio would be selected. So that, the condenser and evaporator heat transfer areas are selected to be 43.52 m^2 and 68.59 m^2, respectively.

The effect of the variation of the motive steam pressure on the TVC system design can be depicted from Fig. 10, which shows the effect of the motive steam pressure on the performance ratio of the thermal vapor compression at different values of boiling temperature.

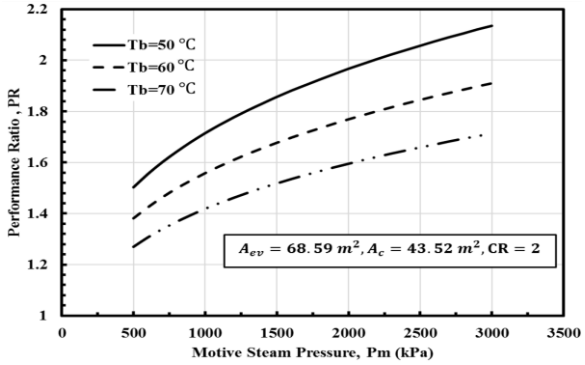

Fig. 12 Effect of the motive steam pressure on the performance ratio at different values of boiling temperature for the selected TVC design conditions.

Increasing the motive steam pressure causing an increase in water productivity as described in Fig. 12, effect of the motive steam pressure on the distilled water at different values of boiling temperature.

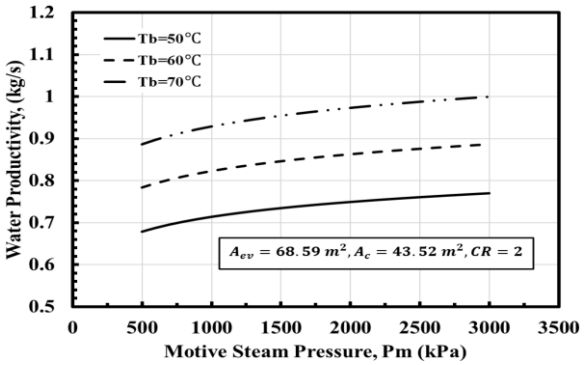

Fig. 13 Effect of the motive steam pressure on the water productivity on the boiling temperature for the selected TVC design conditions.

Secondly, the mathematical model of the DCMD is solved for the conditions presented in Table 2 in order to consume all the heat rejected from the TVC system constrained with that the rejected feed temperature from the DCMD system equals to nearly 35 ℃. The feed temperature of the DCMD module depends on the boiling temperature of the TVC evaporator where the feed solution to the DCMD is the rejected brine from the TVC.

The DCMD model has been analyzed as a function of variation of the boiling temperature in the range of (50 to 70℃) and variation of the motive steam pressure in the range of (500 to 3000 kPa). Figure 14 shows the effect of the variation of the boiling temperature on the permeate flux produced by the DCMD system at different values of motive steam pressures. It is noticed that by increasing the boiling temperature the permeate flux increases. This is due to increasing the inlet feed temperature to the DCMD which enhances the heat and mass transfer through the DCMD module. On the other hand, increasing the motive steam pressure increases the permeate flux due to increasing of the brine mass flow rate from TVC. A schematic diagram of the hybrid desalination system driven by steady heat source is shown in Fig. 15.

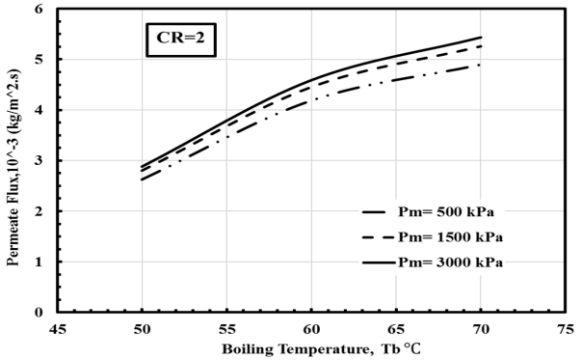

Fig. 14 Effect of the boiling temperature on the permeate flux at different values of motive steam pressure.

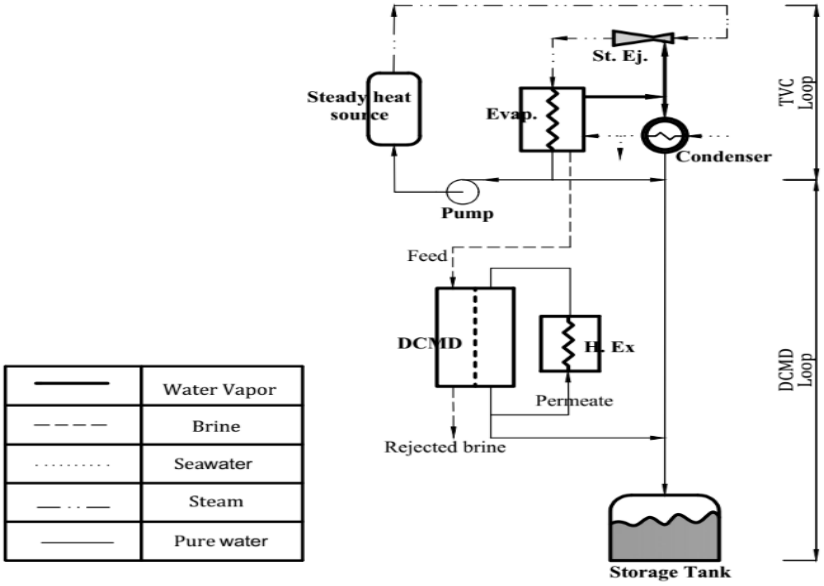

Fig. 15 Hybrid TVC/DCMD system driven by steady state heat source.

Figure 16 presents the effect of variation of the boiling temperature on the DCMD efficiency at different values of motive steam pressure. It can be observed that increasing both the motive steam pressure and boiling temperature increase the efficiency of the system due to the increase in the permeate flux produced.

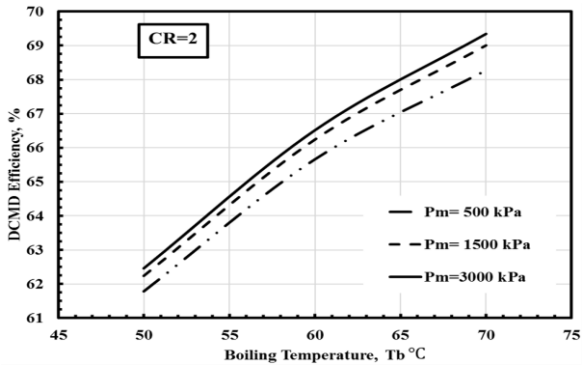

Fig. 16 Effect of the boiling temperature on DCMD efficiency at different values of motive steam pressure.

Figure 17 shows the effect of variation of the motive steam pressure on the water productivity of the hybrid system at different values of boiling temperature compared to the TVC system. It is noticed that, the water productivity from the hybrid system is higher than the water productivity from the TVC system at the same conditions. As a result of increasing the water productivity of the hybrid system than the TVC system, the performance ratio of the hybrid system increases as shown in Fig. 18, which shows the effect of the motive steam pressure on the performance ratio of the hybrid system at different values of boiling temperatures compared to TVC system.

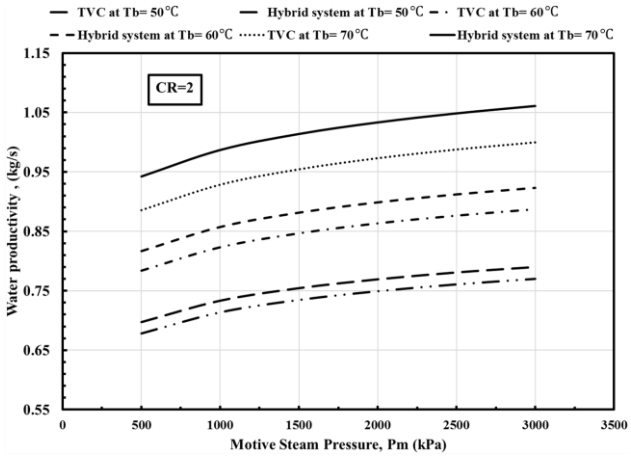

Fig. 17 Effect of the motive steam pressure on the water productivity at different values of boiling temperatures compared to TVC system.

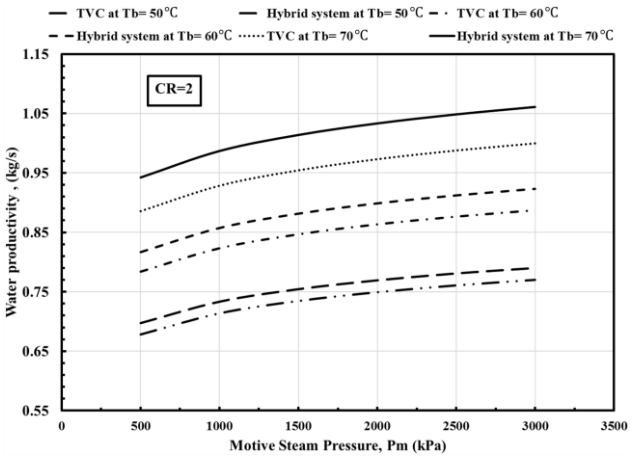

Fig. 18 Effect of the motive steam pressure on the water productivity at different values of boiling temperatures compared to TVC system.

5.2. Hybrid Desalination System Driven by Dynamic Heat Source

From the previous section it is concluded that, the highest water productivity and performance ratio occurred at motive steam pressure of 3000 kPa and boiling temperature of 70 ℃. The present section deals with studying the behavior of the proposed hybrid system using dynamic heat source (PTC) as shown previously in Fig.5. Firstly, the PTC mathematical model is solved using the designed data shown in Table. 6, this solar collector is designed to meet the requirements of the hybrid system from heat.

PTC is designed as the inlet oil "Esso oil" temperature to the PTC is higher than the condensate motive steam temperature T_{mi} by 5 to 6 ℃. Subsequently, the inlet oil temperature to PTC, T_{oi}, is designed to be 90℃. This allows the heat to be transferred from the oil to the condensate motive steam through the heat exchanger. These values of inlet oil temperature, T_{oi}, can be obtained by heating the oil in the morning from 25 ℃ to be 90 ℃, Fig. 19 shows the energy balance on the oil/motive steam heat exchanger.

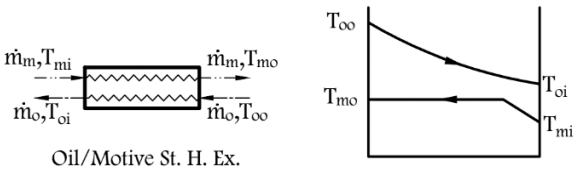

Fig. 19 Energy balance on the oil/motive steam heat exchanger

$$\dot{Q}_{H.ex} = \dot{m}_o * c_{po} * (T_{oo} - T_{oi}) = \dot{m}_m * (h_{mo} - h_{mi}) \quad (60)$$

Where $\dot{Q}_{H.ex}$ is the heat load through the heat exchanger (kW), c_{po} is oil specific heat $(kJ/kg.℃)$, T_{oo} is the oil outlet temperature from the heat exchanger (℃), T_{oi} is the oil inlet temperature to the heat exchanger (℃), h_{mo} is the enthalpy of the outlet motive steam from the heat exchanger $(kJ/kg)$and h_{mi} is the enthalpy of the inlet motive steam to the heat exchanger (kJ/kg).Also, variation of the oil outlet temperature, T_{oo}, results in changing of motive steam mass flow rate through the TVC system which affects the performance of the hybrid system. Firstly, in order to study the dynamic behavior of the hybrid system for different months, the intensity of the solar radiation is set as predicted by Hassan [31].

Approximation polynomial equations for Cairo are used as the input values for the simulation program of PTC for all the four seasons from 8 AM to 4 PM with maximum difference equal to 2%. The values of four season solar intensity are plotted as shown in Fig. 20. The number of PTC collectors to meet the needs of heat input to the hybrid desalination system are 867 collectors.

Variation of the input heat to the heat exchanger at different months of the year with time is represented in Fig. 21. It is concluded that the maximum heat input to the hybrid system is acheived in summer due to the highest values of solar intensity readings but lower heat input happens through winter and autumn due to the low values of solar intensity.

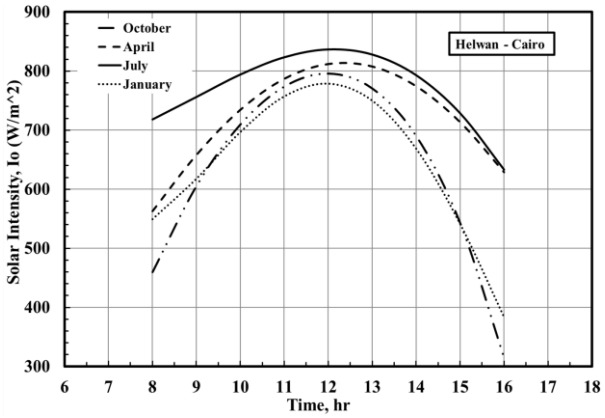

Fig. 20 Variation of solar intensity with time for January, April, July and October.

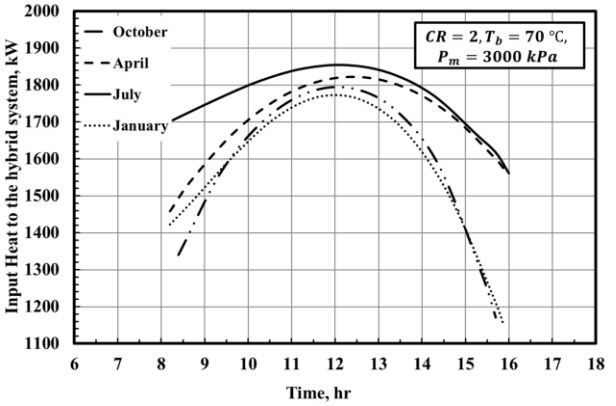

Fig. 21 Variation of the input heat to the hybrid desalination system with time for January, April, July and October.

Figure 22 shows a comparison between the performance ratio of the TVC and the hybrid system with time for the four months. Higher values of performance ratio obtained for the hybrid system for all the four months than that of the TVC system. So, adding the DCMD system enhances the performance ratio for the TVC by 7.3%.

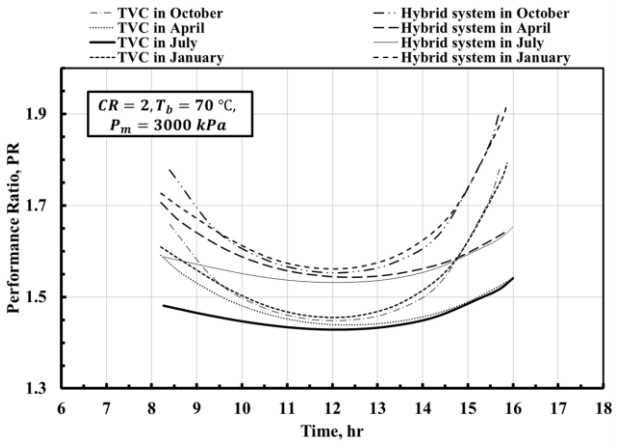

Fig. 22 Variation of the performance ratio of the TVC and hybrid system with time for January, April, July and October

The results of the accumulated water productivity are gathered for each month to know the water productivity for a certain day in that month. The results of the accumulation for dynamic TVC only and dynamic hybrid system are plotted as shown in Fig. 23. It is noticed that higher values of water productivity from the TVC only and from the hybrid system occurred in July which is equal 33.45 and 35.88 ton/day, respectively. Also, the lowest values of water productivity occur in January of 30.03 and 32.19 ton/day.

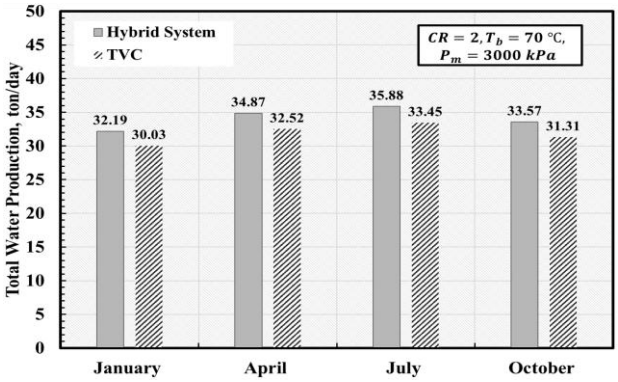

Fig. 23 Accumulated water productivity through a certain day in January, April, July and October

Subsequently, efficiency of the dynamic hybrid system is calculated. The results are plotted in Fig. 24. The efficiency ranges from 45 to 75%, higher values obtained at lower instantaneous solar intensity. Therefore, January has the highest efficiency and July has the lowest one.

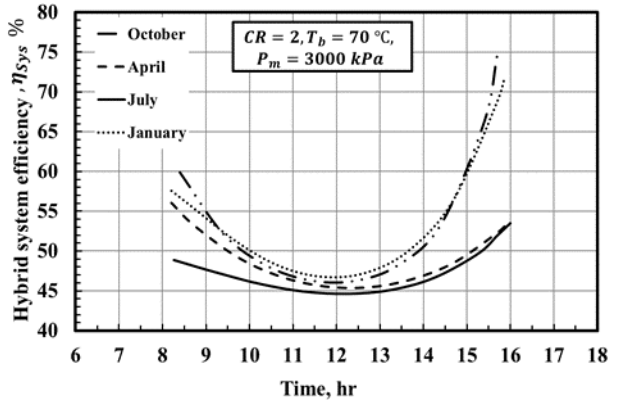

Fig. 24 Variation of the hybrid system efficiency with time for January, April, July, October.

6. COST ANALYSIS

This section is concerned with the evaluation of the cost of the potable fresh water from both the hybrid desalination system (TVC/DCMD) and the stand-alone TVC system using solar energy (PTC). Evaluation of the system's cost based on different economic factors as follows:

The Capital Recovery Factor (CRF), which is the function of the lifetime (n) of the system and the interest rate (r):

$$CRF = \frac{r * (1+r)^n}{(1+r)^n - 1} \quad (61)$$

Therefore, the first annual cost (FAC) is given as:

$$FAC = TIC * CRF \quad (62)$$

Where TIC is the total initial cost of the system components (\$). The initial cost of each component of the dynamic hybrid desalination system were provided from many sources [32], [33], [34], these costs are given in Table 7.

Table 7: Initial costs of the dynamic hybrid system compoenets

Component	IC, \$	Ref.
Solar field	$170 * A_{col}$	[35], [36]
Condenser	$150 * (A_{cond})^{0.8}$	[36], [37]
Evaporator	$1180 * A_{evap}$	[32]
Membrane	$280 * A_m$	[33]
Pumps	$800 * (\dot{W}_P)^{0.47}$	[36], [37]
Heat Exchangers	$150 * (A_{H.ex})^{0.8}$	[36], [37]

The Required oil/motive steam heat exchanger area $(A_{H.ex})$ can be calculated as follows:

$$A_{H.ex} = \frac{\dot{Q}_{H.ex}}{U * LMTD} = \frac{1854 * 1000}{1000 * 30} = 61.8\ m^2 \quad (63)$$

Where $\dot{Q}_{H.ex}$ is the heat load of the heat exchanger (W), U is the overall heat transfer coefficient $(W/m^2.℃)$ and $LMTD$ is the logarithmic mean temperature difference (℃). The Required motive steam pump power $(\dot{W}_p)$ can be calculated as follows:

$$\dot{W}_p = \frac{\dot{m}_m * v * \Delta P}{\eta_p} = \frac{0.86 * 0.001 * 2942}{0.75} = 1.012\ kW \quad (64)$$

Where $\dot{m}_m$ is the motive steam flow rate (kg/s), v is the specific volume of the condensate steam (m^3/kg), ΔP is the pressure difference through the steam pump (kPa), η_p is the polytropic efficiency of the pump. From the following relation the Sinking Fund Factor (SFF) can be calculated from:

$$SFF = \frac{r}{(1+r)^n - 1} \quad (65)$$

Assuming that *50%* of the system components is reusable material, so the Salvage value (S) can be calculated from:

$$S = 0.5 * TIC \quad (66)$$

Then, the Annual Salvage Value (*ASV*) will be equal:

$$ASV = SFF * S \quad (67)$$

The Annual Cost (AC) of the proposed hybrid desalination system can be calculated from the following equation:

$$AC = FAC + O\&MC - ASV \quad (68)$$

So finally, the cost of the potable water per liter can be determined by dividing the Annual Cost (AC) to the Annual Product Yield (AY):

$$Cost/L = \frac{AC}{AY} \quad (69)$$

Different costs of both the hybrid desalination and stand-alone TVC system driven by PTC can be calculated based on Table 8.On the other hand, the final calculations of both the hybrid and the stand-alone TVC systems are given in Tables 9 and 10, respectively. So, it can be concluded that the cost of the water produced by dynamic TVC only is 0.0188 $/ L which is higher than the cost of the potable water produced by dynamic TVC/ DCMD which is 0.0176 $/ L. Therefore, the dynamic hybrid system is more efficient from the economical point of view.

Table 8: Different costs of the system

Plant Life time (n)	20 years
Interest Rate (r)	10%
Plant availability	90%
Annual Product Yield (AY)	12285.9*10^3 L/year
Annual Maintaince Cost (AMC)	15% *FAC [38]
Membrane Replacement Cost (MRC)	20% *Membrane cost [39]
Insurance Cost (IC)	0.5%* FAC [40]
Chemicals Cost (CC)	0.018 $/ m^3 [41]
Spares Cost (SC)	0.033 $/ m^3 [41]
Labor Cost (LC)	0.03 $/ m^3 [39]
Brine Disposal Cost (BDC)	0.015 $/ m^3 [41]

Table 9: Final calculations of cost analysis the hybrid system driven by PTC

Factor	Value
TIC	1,530,000 $
CRF	0.1175
FAC	$179.46 * 10^3$ $
S	765,000 $
SFF	0.0175
ASV	$13.39 * 10^3$ $
AMC	$26.92 * 10^3$ $
IC	630 $
CC	897.3 $
SC	199.03 $
LC	364.89 $
BDC	331.72 $
O&MC	165.86 $
AC	$29.51 * 10^3$ $
AY	$195.58 * 10^3$ $
Cost/L	0.0176 $/L

Figure 25 shows a comparison between the costs of different desalination systems from literature studies as stated by Karagiannis and Soldatos[42] and Tzen [43], it can concluded that the cost of the potable water produced by the dynamic hybrid system (small capacity system) which equal to 0.0176 $/ L (17.6 $/$m^3$) is acceptable value.

Table 10: Final calculations of cost analysis of stand-alone TVC driven by PTC

Factor	Value
TIC	1,520,000 $
CRF	0.1175
FAC	$178.6 * 10^3$$
S	$760 * 10^3$$
SFF	0.0175
ASV	$13.3 * 10^3$$
AMC	26790 $
IC	893$
CC	185.62 $
SC	340.3 $
LC	309. 4 $
BDC	*154.68 $*
O&MC	*28,673 $*
AC	$193.973 * 10^3$$
AY	11457.9*10^3 L/year
Cost/L	0.0188 $/L

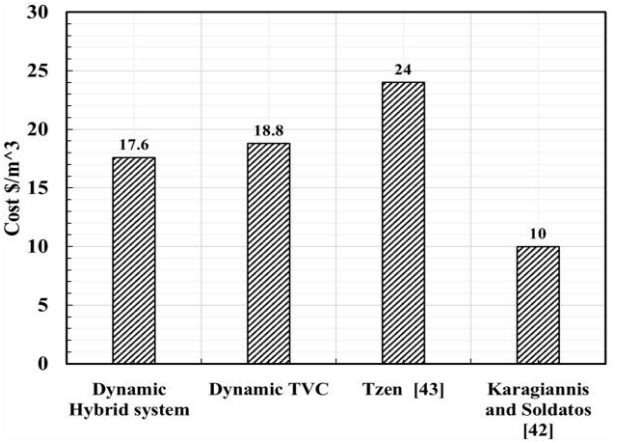

Fig. 25 Comparison between Dynamic TVC cost, Dynamic hybrid system cost and costs from Literature Survey.

7. CONCLUSION

This study presented a thermal and economic analysis of a hybrid desalination system consists of thermal vapor compression and direct contact membrane distillation system using parabolic trough collectors as a heat source.

The results showed that both of the performance ratio and water productivity enhanced by 7.3% by adding the DCMD as a secondary desalination unit. In addition, the hybrid system efficiency reached to 75%.

Since, the cost of the fresh water product by dynamic TVC only is 0.0188 $/ L which is higher than the cost of the potable water produced by dynamic TVC/ DCMD which is 0.0176 $/ L. Therefore, from the economical point of view the dynamic hybrid desalination (TVC/DCMD) system is more efficient than the dynamic stand-alone TVC system.

8. LIST OF SYMBOLS

a	Thermal diffusity = $k/\rho.c_p$,	m^2/s
ab	Absorptivity	
B	Permeability,	$kg/m^2.s.Pa$
BPE	Boiling point elevation,	℃
CF	Concentration factor,	
c_p	Specific heat at constant pressure, $kJ/kg.K$	
h	Heat transfer coefficient, Enthalpy, $kW/m^2.℃, kJ/kg$	
I_o	Solar intensity,	W/m^2
J	Permeate flux,	$kg/m^2.s$
k	Thermal conductivity,	$kW/m.℃$
M	Molecular weight,	kg/kmole
$\dot{m}$	Mass flow rate,	kg/s
n	Life time,	years
O&MC	Operating and Maintenance Cost,	$
PCF	Pressure correction factor,	kPa
PD	Diffusivity of water vapor,	m^2/s
$\dot{Q}$	Heat transfer rate,	kW
r	Radius, Interest rate,	m, %
R	Universal Gas constant,	$kJ/kmole.K$
S	Salinity, Salvage value,	g/kg, $
t	Time	hr
TCF	Temperature correction factor,	℃
U	Overall heat transfer coefficient	$kW/m^2.℃$
V	Velocity,	m/s
w	Width,	m
$\dot{W}$	Power,	kW
x	Salinity,	ppm
ΔH	Latent heat of vaporization,	kJ/kg
α	Combined heat transfer coefficient of convection and radiation,	$kW/m^2.℃$
γ	Correction factor of diffuse radiation	
δ	Membrane thickness,	
λ	Latent heat	$kJ/kg, m$
τ	Transmissivity, tortuosity,	
ε	Porosity,	%
σ	Stefan Boltzmann constant,	$W/m^2.K^4$

Subscripts

a	ambient
b	Brine or boiling
bf	Bulk feed
bp	Bulk permeate
c	Condenser, condensate or conduction
col	Collector
col	Collector
conv	Convection
cw	Cooling water
d	Distillate
e	Evaporator
egc	Effective
ev	Entrained vapor
f	Feed, fluid
g	Glass envelop
H.ex	Heat exchanger
hy	Hybrid system
i	Inlet, inner
m	Motive steam or membrane or mean
md	Membrane distillation
o	Outlet, outer
p	Pore or permeate
PTC	Parabolic trough collector
r	Receiver
rad	Radiation
s	Heating steam
sys	System
v	Vapor
w	Water vapor

9. REFRENCES

[1] Al-Juwayhel,F., El-Dessouky, H., and Ettouney, H. , 1997, "Analysis of single-effect evaporator desalination systems combined with vapor compression heat pumps," Desalination, VOL. 114, pp. 253–275.

[2] Darwish, M. and El-Dessouky,H., 1996, "The heat recovery thermal vapour-compression desalting system: A comparison with other thermal desalination processes," Desalination, VOL. 16, No. 6, pp. 523–537.

[3] Hamed, O., Zamamiri,O., Aly, S., and Lior, N. , Apr. 1996, "Thermal performance and exergy analysis of a thermal vapor compression desalination system," Energy Convertions Management, VOL. 37, No. 4, pp. 379–387.

[4] Han, B., Liu, Z., Wu, H., and Li, Y.,2014 "Experimental study on a new method for improving the performance of thermal vapor compressors for multi-effect distillation desalination systems," Desalination, VOL. 344, pp. 391–395.

[5] Alkhudhiri, A., Darwish, N. and Hilal N., 2012, "Membrane distillation : A comprehensive review," Desalination, VOL. 287, pp. 2–18.

[6] Schofield, R., Fane, A., Fell, C., and Macoun, R., Mar. 1990 ,"Factors affecting flux in membrane distillation," Desalination, VOL. 77, pp. 279–294.

[7] Termpiyakul, P. and Jiraratananon, R.,2005, "Heat and mass transfer characteristics of a direct contact membrane distillation process for desalination,", Desalination, VOL. 177, pp. 133–141.

[8] Khayet, M., Velázquez, A. and Mengual, J. , Jan. 2004, "Modelling mass transport through a porous partition: Effect of pore size distribution," Journal of Non-Equilibrium Thermodynamics., VOL. 29, No. 3, pp. 279–299.

[9] Drioli, E., Laganà, F., Criscuoli, F.,and Barbieri, G., 1999"Integrated membrane operations in desalination processes," Desalination, vol. 122, no. 2–3, pp. 141–145.

[10] Hamed,O.,2005, "Overview of hybrid desalination systems - Current status and future prospects," Desalination, VOL. 186, No. 1–3, pp. 207–214.

[11] Kalogirou,S., 2004, "Solar thermal collectors and

applications," Progress in Energy Combustion Science., VOL. 30, No. 3, pp. 231–295.

[12] Suman, S., Kaleem Khan,M. and Pathak, M., , 2015, "Performance enhancement of solar collectors—A review," Renewable Sustainable Energy, VOL. 49, No. 49, pp. 192–210.

[13] Fernández-García, A., Zarza, E.,Valenzuela, L., and M. Pérez, 2010, "Parabolic-trough solar collectors and their applications," Renewewable Sustainable Energy, VOL. 14, No. 7, pp. 1695–1721.

[14] Mohamed,A.M, 2003, "Numerical investigation of the dynamic performance of parabolic trough solar collectors using different working fluids," Port Said Engineering Journal., VOL. 7, No. 1, pp. 100–115.

[15] Govind and Tiwari, G. N., 1984, "Economic Analysis of Some Solar Energy Systems," Energy Convertions. Managment., VOL. 24, No. 2, pp. 131–135.

[16] Elminshawy, N. A., Mohamed, A. M. I., and Kassem, M., 2011, "Desalination System Powered By a Hybrid Waste Heat and Solar Energy," in Sustainable Energy Technologies, pp. 4–7.

[17] El-Dessouky, H. and Ettouney, H., Fundamentals of salt water desalination. Kuwait: Elsevier Science, 2002.

[18] El-dessouky. H., and Ettouney, H., 2010, "Single-Effect Thermal Desalination Process: Thermal analysis," Heat Transfer Engineering, VOL. 20:2, pp. 52–68.

[19] El-Dessouky, H., and Ettouney, H.,1999, "Multiple-effect evaporation desalination systems. thermal analysis," Desalination, VOL. 125, No. 1–3, pp. 259–276.

[20] "www.OakaleEngineering.com,"

[21] Bin Amer, A., 2011, "New Trend in the Development of ME-TVC Desalination System," in Desalination, Trends and Technologies, M. Schorr, Ed. India: InTech open Acess.

[22] Bin Amer, A., Dec. 2009, "Development and optimization of ME-TVC desalination system," Desalination, VOL. 249, No. 3, pp. 1315–1331.

[23] Çengel, Y. ,2002," Heat and Mass Transfer: A practical approach", 2 nd ed. New York, McGraw-Hill..

[24] Khayet, M. and Matsuura, T. ,2011,"Membrane distillation principles and applications", 1 st ed. Elsevier.

[25] Bahmanyar, A., Asghari, M., and Khoobi, N., 2012, "Numerical simulation and theoretical study on simultaneously effects of operating parameters in direct contact membrane distillation," Chemical Engineering and Processing., VOL. 61, pp. 42–50.

[26] Qtaishat, M., Matsuura, T., Kruczek, B. and Khayet, M. , Jan. 2008, "Heat and mass transfer analysis in direct contact membrane distillation," Desalination, VOL. 219, No. 1–3, pp. 272–292.

[27] Schofield, R. W., Fane, A., and Fell, C., Oct. 1987, "Heat and mass transfer in membrane distillation," Journal of Memberane Science, VOL. 33, No. 3, pp. 299–313.

[28] Phattaranawik,J.,Jiraratananon, R. and Fane, A. , 2003, "Heat transport and membrane distillation coefficients in direct contact membrane distillation," Journal of Memberane Science., VOL. 212, pp. 177–193.

[29] Khayet, M., Matsuura, T., and Mengual,J., 2005, "Porous hydrophobic/hydrophilic composite membranes: Estimation of the hydrophobic-layer thickness," Journal of Membrane Science., VOL. 266, No. 1–2, pp. 68–79.

[30] Bui, V., Vu, L., and Nguyen, M., 2010, "Modelling the simultaneous heat and mass transfer of direct contact membrane distillation in hollow fibre modules," Journal of Membrane Science, VOL. 353, No. 1–2, pp. 85–93.

[31] Hassan, A. , 2001 ,"The variability of the daily solar radiation components over Helwan," Renewable Energy, VOL. 23, No. 3–4, pp. 641–649..

[32] "http://www.matche.com/equipcost,"

[33] Alklaibi, A. and Lior, N. , 2004, "Membrane-distillation desalination : status and potential," Desalination, VOL. 171, pp. 111–131.

[34] http://www.mhhe.com/engcs/chemical/peters/data/ce.html,"

[35] Jaramillo, E., Venegas-Reyes, J., Aguilar, O., Castrejón-García, R. and Sosa-Montemayor, F., 2013, "Parabolic trough concentrators for low enthalpy processes," Renew. Energy, VOL. 60, pp. 529–539

[36] Sharaf, M., Nafey, A. and García-Rodríguez,L., 2011, "Thermo-economic analysis of solar thermal power cycles assisted MED-VC (multi effect distillation-vapor compression) desalination processes," Energy, VOL. 36, No. 5, pp. 2753–2764.

[37] Voros,N., Kiranoudis, C. and Maroulis, Z., 1998 "Solar energy exploitation for reverse osmosis desalination plants," Desalination, VOL. 115, No. 1, pp. 83–101.

[38] Kabeel, A., Hamed, A., and El-Agouz, S.,2010, "Cost analysis of different solar still configurations," Energy, VOL. 35, No. 7, pp. 2901–2908.

[39] Macedonio, F., Curcio, E., and Drioli, E., 2007, "Integrated membrane systems for seawater desalination: energetic and exergetic analysis, economic evaluation, experimental study," Desalination, VOL. 203, No. 1–3, pp. 260–276.

[40] Ettouney,H., El-Dessouky, H., Faibish, R., and Gowin, P., 2002, "Evaluating the economics of desalination," Chemical Engineering Progress, VOL 98, No. 12, pp. 32–39.

[41] Al-obaidani, S., Curcio, E., Macedonio, F., Di, Al-hinai, H. and Drioli, E., 2008, "Potential of membrane distillation in seawater desalination : Thermal efficiency , sensitivity study and cost estimation," Journal of Memberane Science., VOL. 323, pp. 85–98.

[42] Karagiannis, I., and Soldatos,P., 2008, "Water desalination cost literature: review and assessment," Desalination.

[43] Tzen, E. and Morris, R., 2003,"Renewable energy sources for desalination," Solar Energy, VOL. 75, No. 5, pp. 375–379.